INTERNATIONAL JOURNAL OF
COASTAL & OFFSHORE ENGINEERING
IJCOE Vol.4/No. 1/Spring 2019 (21-29)

Available online at: http://ijcoe.org/browse.php?a_code=A-10-269-1&sid=1&slc_lang=en

Numerical Modeling of Wave and Current Patterns of Beris Port in East of Chabahar-Iran

Mesbah Sayehbani[1*], Danial ghaderi[2]

[1] *Assistant Professor, Department of Marine Engineering, Amirkabir University of Technology, Bandar Abbas, Iran, msaybani@aut.ac.ir*
[2*] *Ph.D. student, Faculty of Marine Science and Technology, University of Hormozgan, Bandar Abbas, Iran; danialghaderi1@gmail.com*

ARTICLE INFO

Article History:
Received: 22 Feb. 2019
Accepted: 22 May 2019

Keywords:
Breakwater
Oman Sea
Beris port
MIKE21

ABSTRACT

The wave and current patterns of the Beris port and its surroundings before and after construction of the breakwater structure was investigated by numerical model, MIKE 21. For this purpose, the required data was provided and the model was prepared for implementation within a month from July 22 to August 21, 2016. In order to verify the modeling results, the extracted data were compared with the data derived from the global wave model; WAVEWATCH III and ECMWF. The simulation results show the significant effect of the breakwater on the stillness of the basin and the change in flow direction. According to the position of the port and the morphology of the coast, is expected to parallels sedimentation caused by waves and currents of the region focused on the long arm breakwaters and adjacent to the entrance mouth of breakwaters, as well as in the coastal part of the small arm of the breakwater.

1. Introduction

The coastal zone is one of the most dynamic regions that are affected by various parameters such as waves, currents and storms. On the other hand, this zone has always been exploited by human beings. In order to manage and control such a region and the structures constructed therein such as ports, hydrodynamic study of the region is essential. In the present study, we have tried to investigate the patterns of wave, current and sedimentation around the Beris Fishing Port in the East of Chabahar Port. Since reliable data and validated sampling are necessary for such studies, it has been tried to study the hydrodynamic conditions of the region by numerical modeling using existing and available data from global atmospheric and wave models.

The wind plays a major role in the formation and propagation of waves, so that ocean waves with different spatial and temporal scales as well as coastal waves are all strongly influenced by wind [1]. Today, the third-generation numerical models allow historical studies and prediction of various water areas. Physical and numerical models are two main methods available for simulating the wave propagation or the interaction between waves and marine structures in the coastal engineering [2]. A calibrated and validated model can be a suitable basis for short- and long term studies [1]. With advances in the field of computers and such numerical models, human knowledge of the waves and currents of the seas have now grown considerably, and this feature can partially resolve the prerequisites of hydrodynamic studies. Nowadays, numerical models are the first step in climate change and energy research. [3]. The wave models can be divided into two distinct categories of ocean waves (large scale) and coastal waves (small scale). While most models can be applied to both large and small amplitude, factors such as limitations in computing, efficiency and accuracy determine their use. Numerical models of ocean known as; WAM [4], WW3 [5], and coastal-like; SWAN [6], MIKE21-SW [7] and TOMAWAC [8]. It should always be noted that its crucial point lies in the evaluation of the model inputs according to its outputs, including boundary conditions and physical parameters such as white capping, wave breaking and bottom friction [9].

One of the main problems of Iranian ports, after construction, is the sedimentation problem that occurs in the entrance of the port and then proceeds to the main basin, which disrupts the vessel traffic and ultimately results in inefficiencies of the ports. A study on the northern coasts of the Gulf of Oman on the wave and current pattern of the Ramin Port (near the study area of this research) was carried out by Isaie Moghaddam et al. 2018, that shows, that coastal currents flow to the port minor basin and form cyclonic genres that

contribute in carrying and depositing coastal sediments inside the port basins [10]. Beris port is also facing this problem, and dredging operations with high costs are carried out annually to overcome this problem [11]. Although several studies have already been done on sedimentation in this port, in this research we have tried to study wave and current patterns by numerical model using available data and global models of wind and current, and interpret the sedimentation processes by using the obtained results.

2. Materials and methods

The patterns of wave and current were simulated by using a software package of MIKE21 for the coastal part of the Oman Sea in the vicinity of Beris port, As with other similar studies using this software package [12]. In this numerical simulation by MIKE21/3 Coupled Model FM, the wave module (SW) and the current module (HD) have been used.

2.1 The Study Region

The study area in this research is Beris fishery harbor, located in southeast of Iran, along the northern coasts of the Gulf of Oman at 25.147° N latitude and 61.176° E longitude (figure 1A), This fishing port is located 85 km east of Chabahar city. Beris port is composed of two breakwaters, so that the main breakwater (The big one) is located on the extent of coastal nose along south-north direction, and the subsidiary breakwater (The small one) has been constructed along east-west direction. figure 1B shows the coastline changes around the port of Beris during 1994 and 2016, With the visual interpretation of aerial images, well-defined areas affected by sedimentation. It is therefore predictable that the major sediment is in the subsidiary breakwater (The small one).

2.2 Numerical model

Among the most popular numerical models for analyzing the phenomena governing the marine environment, the MIKE mathematical model developed by the Danish Hydraulic Institute is well-known and widely used software [7]. This modeling software has the capability of simulating phenomena in one, two and three dimensions in all aquatic environments, including estuaries, coastal areas, seas and oceans [4]. Various features of this numerical model for receiving input data in a wide range and providing graphical outputs suitable for research and engineering needs make it an appropriate tool for simulating and analyzing phenomena such as wave and current patterns, sedimentation and erosion in coastal regions, and determining the transfer rate of coastal sediments [13]. In this study, the SW and HD modules of MIKE21 software package was used to simulate wave and current patterns.

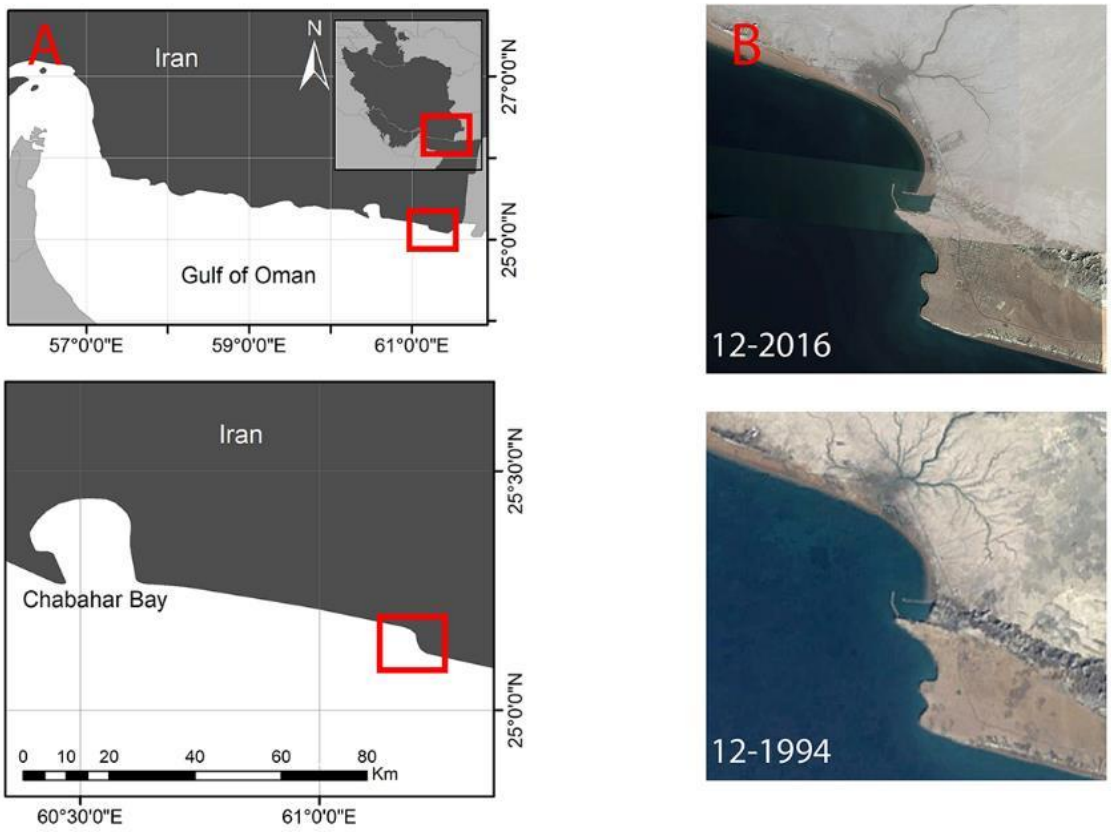

Figure 1: A: Location of the Beris Port, relative to Iran and the Gulf of Oman.
B: Aerial view of the Beris fishing port during 1994-2016

Table 1: The selected domain and its specifications for numerical modeling

Mesh	Mesh environment	Latitude (N)	Longitude (E)
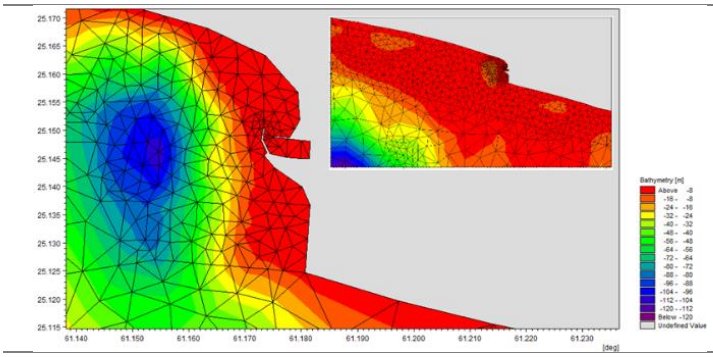	1	24.84495	60.59340
	2	25.29640	60.59340
	3	25.29640	61.37414
	4	24.84495	61.37414
	Nodes/ Elements	2030/3789	

Therefore, according to the region under study, a region with the specifications listed in Table 1 was selected for simulation. This region was discretized to 2030 nodes and 3789 elements using an unstructured mesh, which was made up of coarser mesh in the zone far from breakwater and finer meshes in the zone near the breakwater (Table 1). Using a coarser mesh in the overall domain of the model is to reduce computational time. To create bathymetry file, the topography data of SRTM + 30 version 6.0 was used, which is referred to USGS EROS institute [14]. Also, the study region has 4 boundaries, so that the northern boundary is considered as land border and the eastern, western, and southern boundaries as water borders.

In the hydrodynamic module, tidal data in the form of water level were introduced as boundary data for the western boundary of the model (figure 2). For eastern and southern boundaries, a fixed value was used because of the absence of a measurement station. Also, for the spectral wave model, the first wave level parameter (Wave parameters (version 1)) was used at all three boundaries. In order to apply the atmospheric conditions to the region, the ECMWF-ERA40 wind data has been used (figure 2), so that the wind speed and direction data from July 22, 2016 for one month was considered for the entire study region in a form of a file with a three-hour time step. In order to study the wave and current conditions of the region, first the numerical model was implemented without the presence of the breakwater, and the model was calibrated in comparison with the data of WW3 and ECMWF global wave models by using the parameters of white capping, wave breaking and bottom friction. It should also be noted that in order to create close-to-reality conditions, the wave-current coupling was used in the simulations. After the model was appropriately calibrated, it was implemented in the presence of the Beris' breakwater. In Table 2, the input parameters of the model are expressed.

WW3 global wave model is a prediction model with a 0.5 degrees accuracy, which is available by the University of Hawaii based on the GFS wind data with one-hour time step from 2010. The WW3 is an open source model developed by NOAA and NCEP [15], which is well validated for deep water and widely used around the world [16]. It is also used for nearshore areas [17].

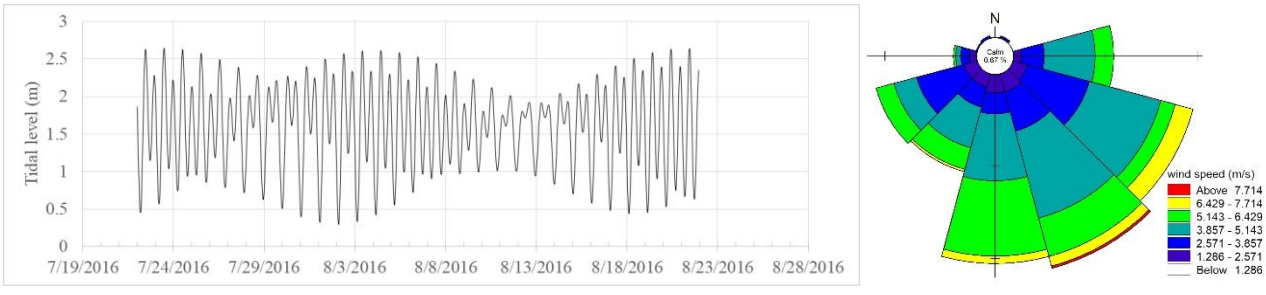

Figure 2: The water level data of Chabahar port and wind roses of the region, extracted from ECMWF-ERA40

Table 2: Parameters used in modeling of the study region

Module	Applied in this investigation	Equations	#
SW/HD	1 Spectral formulation-fully spectral formulation 2 Time –unsteady formulation	Basic Equations	**1**
SW	Dissipation coefficient (cdis=4.5 and Delta=0.5)	White capping	**2**
SW	Gamma data with the value of 0.8 The calibration constant factor,(alpha= 1)	Wave breaking	**3**
SW	Nikuradse roughness =0.04	Bottom friction	**4**
SW/HD	Quadruplet-wave interaction	Energy transfer	**5**
SW	Data from ECMWF institute	Wind forcing	**6**
HD	Tidal level of Chabahar Port	Water level conditions	**7**
SW/HD	SRTM+30	Bathymetry	**8**
HD	The Smagorinsky formulation= 0.28	Eddy viscosity	**9**
HD	Wave Radiation	Wave Radiation	**10**
HD	Chezy number= 32	Bed Resistance	**11**

2.3 Verification of the numerical model

In order to verify the present model, the results of the model were compared with WW3 and ECMWF wave model data at geographic coordinates of 61° E longitude and 25° N latitude [17; 18]. Using calibration coefficients, the numerical results have been tried to be more consistent with the two basic models. As shown in Table 3, in four steps of implementation of the model with the white capping coefficients of 4.5 and 2 and wave breaking coefficients of 0.8, 1, and 0.5, The model with code 1 has the lowest error percentage relative to data of WW3 model as well as ECMWF model. Given the bias statistical index indicating the difference between the mean of the baseline data and the output data of the model (the closer to zero, the higher the accuracy of the model), the index for the model with code 1 has a smaller value than the other models, compared to WW3 and ECMWF models [19]. Also, the model with code 1 shows a better treatment in term of Root Mean Square Error and scatter index , indicating the dispersion rate of the variables relative to the baseline variables and the absolute dispersion of the two variables, respectively. The results of model with code 1 (RUN1) compared with global model data have been shown in figure3. WW3 and ECMWF data are in agreement together, But RUN1 is different. The reason for this difference is the larger mesh in the area, due to the distance from the studied port in order to save time, the model computing network is considered to be larger.

Table 3: Statistical Indicators for verification of the model with different coefficients, against global wave models

	Run1 White Capping =4.5 Wave Breaking =0.8	Run2 White Capping =2 Wave Breaking =0.8	Run3 White Capping =2 Wave Breaking =1	Run4 White Capping =2 Wave Breaking =0.5
% Error WW3	2.16	5.18	6.35	6.24
% Error ECMWF	3.82	6.89	8.08	7.97
Bias WW3	-0.041	-0.100	-0.122	-0.120
Bias ECMWF	-0.072	-0.130	-0.153	-0.151
RMSE WW3	0.280	0.300	0.292	0.299
RMSE ECMWF	0.207	0.241	0.239	0.240
SI WW3	14.52	15.57	15.15	15.54
SI ECMWF	10.74	12.52	12.43	12.45

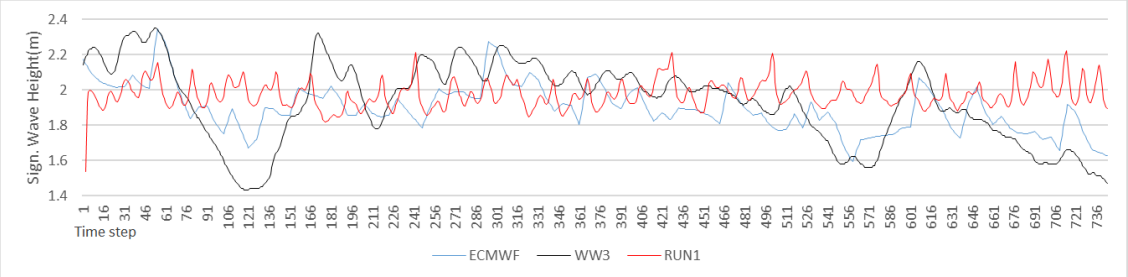

Figure 3: The results of model with code 1 (RUN1) compared with global model data, WW3 and ECMWF

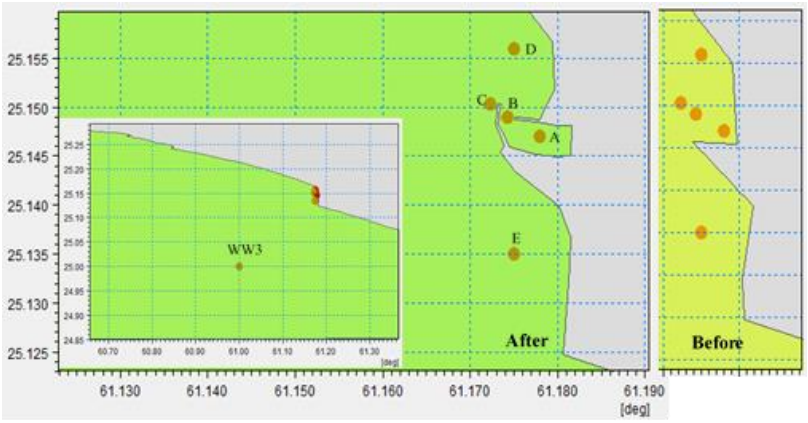

Figure 4: The position of the selected points for comparison of results of model.

3. Results

In order to examine the model of the study region, five points were selected within the basin, at the mouth of the port, behind the major arm of the port, and at upstream and downstream of the port (figure 4). The coordinates of the selected points shown in table 4. After extraction of the data at these points, the necessary analyzes have been done to determine the wave and current patterns as well as prediction of the sedimentation pattern.

3.1 Results of SW model

A view of the overall direction of wind-generated waves in the study region is shown in figure 5. According to this figure, the dominant direction of wind-generated waves is from southwest, as expected.
Diagram of wave heights and Wave roses have been extracted in five-point that shon in figure 6 and table 5. As it is obvious, at the points A and B, which are respectively located within basin and mouth of the port, the wave height has significantly decreased compared to non-presence of the breakwater arm. At point A, the wave height in the absence of the breakwater arm is equal to the average value of 0.62 m and maximum value of 0.8 m, while the average value of wave height in the presence of breakwater arm is 0.01 m. Also, at the point B, the average wave height is 0.68 m, and it reaches to 0.05 m after construction of the port. The wave direction has also significantly changed due to the construction of the Beris port of, so that, in the normal conditions, the wave directions are often from the southwest, and after the construction, they are from the mouth of the breakwater as the only way (Table 5).
In the area behind the breakwater arm (point C), the wave height is about 0.95 m. After the construction of the port, only the dissipation rate of the high velocities has decreased (Table 5).
The wave height at the point D, located outside and at the upper part of the port, a 10.8 percent drop in wave height is observed after the presence of the Beris breakwater and reached to and average height of 0.7 after construction of the port. Also, the wave direction in this area is slightly shifted from southwest to the west, indicating the transport of the sediment particles to the back of the minor arm of the Beris breakwater.
At the point E which is located away from the port, as expected, no change was created in the height and direction of the waves by constructing the port, and the average wave height is about 1.3 m.

Table 4: The coordinates of the selected points for extracting the data from the model and comparing it with the data of the global wave model

Output of points	Latitude (N)	Longitude (E)
WW3/ECMWF	25	61
A	25.147	61.178
B	25.149	61.1743
C	25.1503	61.1723
D	25.156	61.175
E	25.135	61.175

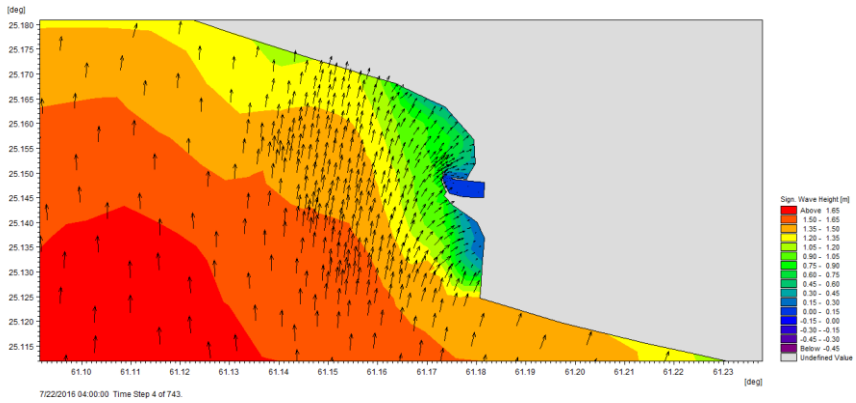

Figure 5: The dominant direction of wind-generated waves near the fishing port; results of SW model

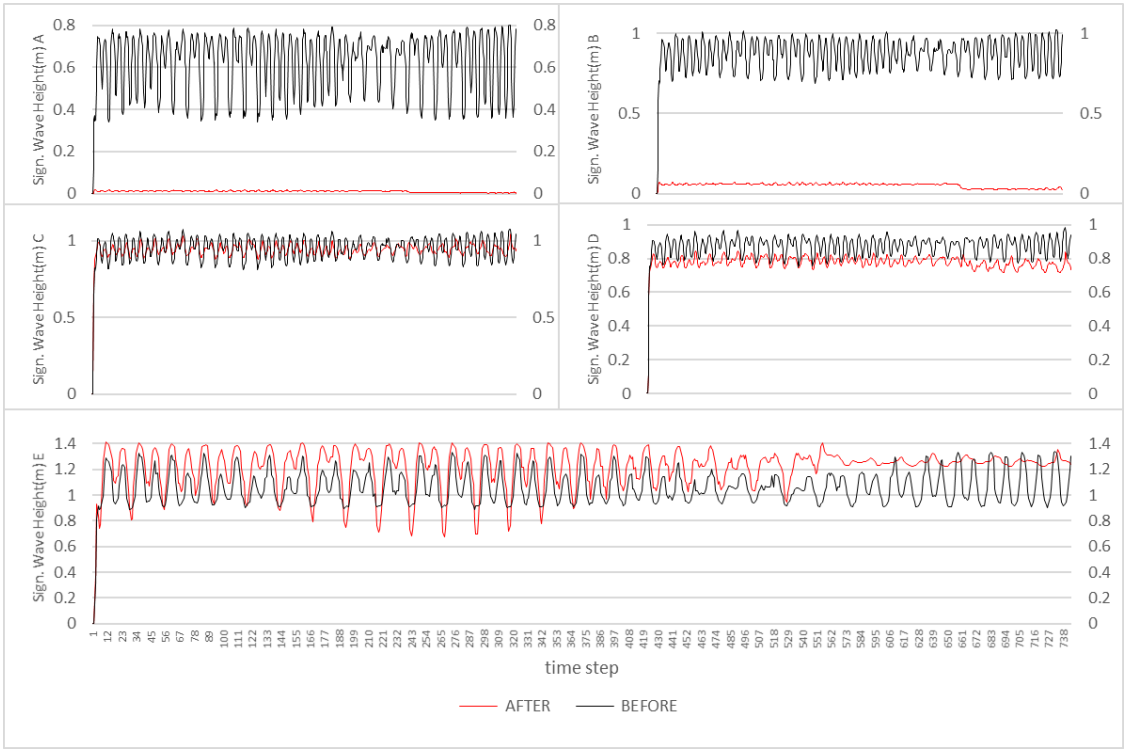

Figure 6: Diagram of wave heights at the five selected points of the port and its surroundings, before and after the construction of the port; results of SW model

Table 5: Wave roses of the selected points of the port and its surroundings, before and after the construction of the port, results of SW model

Point A		**Point B**	
After	Before	After	Before
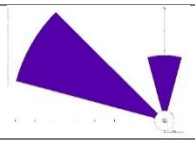	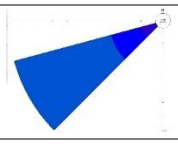	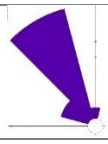	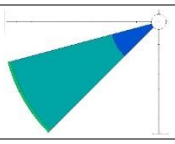
Point C		**Point D**	
After	Before	After	Before
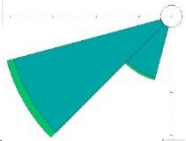		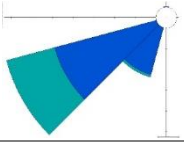	
Point E		**Color Legend**	
After	Before		
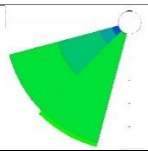	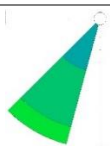	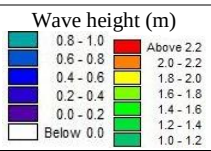	

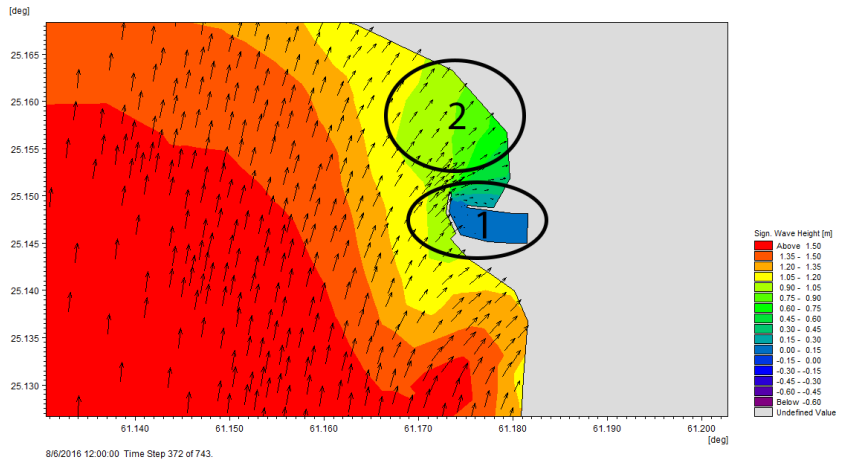

Figure 7: A view of the patterns of wave height and direction around the Beris port; results of SW model

As noted earlier, the direction of dominant waves is from the southwest. This is well illustrated in figure 7, which is related to the time step 372 of the model. According to the figure, the wave height in the port is noticeably low, as expected (the zone 1 in figure 7). Another point to note is that the wave height decreases in the upstream of the port (the zone 2 in Fig. 7), which reduces the water turbulence and therefore can provide a good environment for deposition of sediments.

3.2 Results of HD model

A view of the overall current direction in the Beris port and its surroundings has been shown In figure 8. Accordingly, the dominant current direction is from east to west, which is consistent with the current pattern of the Persian Gulf and Oman Sea. With respect to the coastal morphology, the current direction is changed to be along the coast after reaching the Beris port, and flow includes small circulations and vortices during crossing the Beris breakwater and its upper part (point D).

The results of the HD model representing the current speed are shown in Table 4. As can be seen, at the point A and B, after the construction of the port, the current speed has decreased by 84.3 and 52.4%, and reached from average values of 0.4 m/s and 0.6 m/s to 0.006 m/s and 0.02 m/s respectively.

In the zone behind the breakwater arm (point C), the change in current speed is about 11% and the average speed reaches from 0.05 m/s to 0.06 m/s, which shows the effect of breakwater on the current speed of this area. Also, some vortices forms in this area after the construction of the port and the breakwater arm.

At point D, located in the upper part of the port, the change in current speed is about 27.8% and a decrease from 0.09 m/s to 0.05 m/s is observed.

At point E, unexpectedly, the current speed is increased from an average value of 1.4m/s to 2.6 m/s after construction of the port. Although this increase is unexpected, it can be due to the changes in computational mesh after the inclusion of the port and its arms in the numerical model.

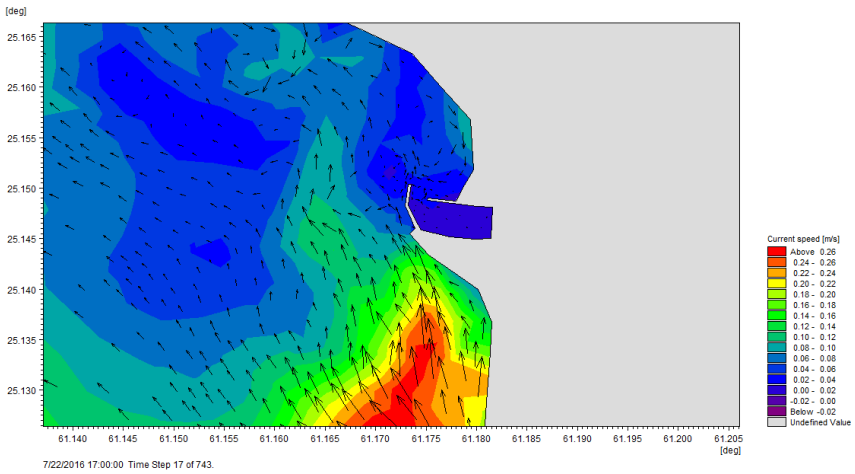

Figure 8: The dominant current direction near the fishing port; the results of HD model

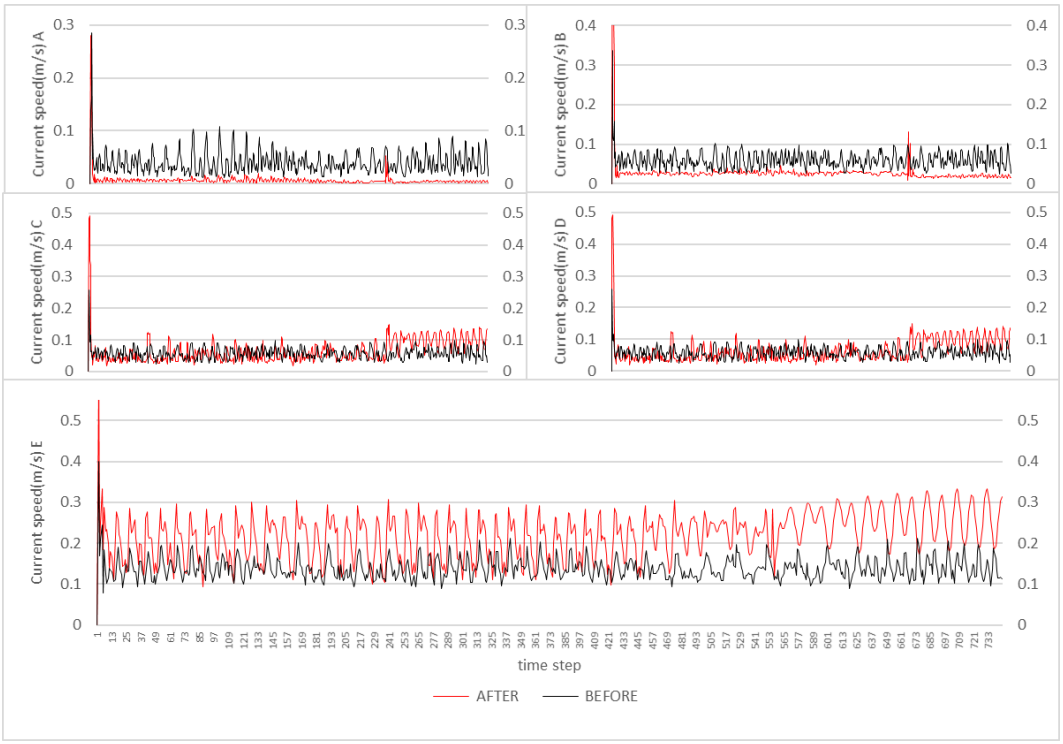

Figure 9: The diagram of current speed at the five selected points of Beris port and its surroundings, before and after construction of the port; results of HD model

The current direction in the study region is toward the west (figure 9), and as seen in figure 10, around Beris port, the current direction is parallel to the coast and toward the head of breakwater (the zone 3 in figure 10). In this region, the current speed decreases rapidly, and some vortices are also formed behind and at the head of the breakwater arm due to the existence of this arm. Inside the port and the inner basin, due to the presence of primary and secondary arms of breakwater, the current speed is extremely low, as shown in the part 1 of figure 10. Another important region is the zone 2 in figure 10, in which the current is often accompanied by a clockwise rotation due to the structure of the coast and the construction of the Beris port. This current has a higher speed at northern part of zone 2 and a lower speed at southern part of zone 2 which is located in the vicinity of the mouth of breakwater.

4. Conclusion

According to the obtained results of wave and current patterns around the Beris fishing port and analysis of these results, one can get an understanding of the general pattern of sedimentation in this port. Also, the present model and verification method used are in a good agreement in comparison with the other studies carried out on this port.

The construction of the Beris breakwater has caused the wave height to decrease in the upper part of the port and the wave directions, which are often from the southwest, to be slightly oriented toward west and guided to the behind of the minor arm of breakwater.

Consequently, suitable conditions for penetration of sediments to the region located in the vicinity of the mouth of breakwater are provided. Also, there is a

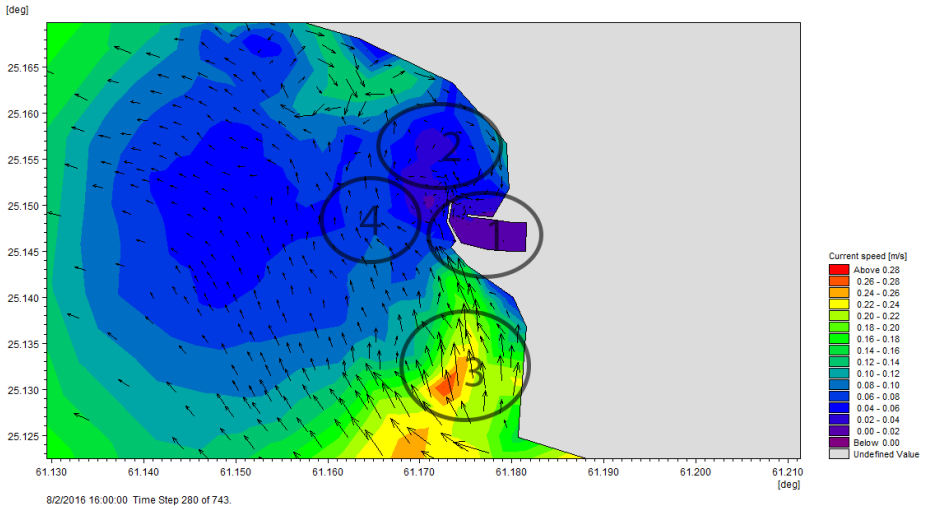

Figure 10: A view of current speed and direction around the Beris port, results of HD model

clockwise current in this region that can transport sediments to the behind of the minor arm of breakwater. Due to the low current speed in this region, a considerable amount of sediment is accumulated in the long run. This issue can be confirmed by comparing satellite images from previous years.

In the region behind the major arm of breakwater, the current speed is generally increased in comparison with the absence of a breakwater, which indicates the effect of this structure on the current pattern of the region. The current speed is higher at the lower part of the Beris port and is parallel to the coastline toward the behind of the major arm. This speed is suddenly drops and causes all sediments, transported to the lower part of the port, have the opportunity to be deposited behind the major arm of Beris port. Therefore, the port encounters a sediment problem at the head of the breakwater, which this sediment can then be transferred into the basin.

5. Acknowledgments

In this way, the authors of the paper express their gratitude and appreciation for the Management of Hydrographic and Tidal Iran Mapping Organization, for the use of the tidal data and the University of Hawaii for the use of world wave model data, WW3.

References

1- Reguero, B. G., Losada, I. J., & Méndez, F. J. (2015). *A global wave power resource and its seasonal*, interannual and long-term variability. Applied Energy, 148, 366-380.

2- Yang, Z. W., Liu, S. X., & Li, J. X. (2014). *An improved coupling of numerical and physical models for simulating wave propagation*. China Ocean Engineering, 28(1), 1-16.

3- Janssen, P. A. (2008). *Progress in ocean wave forecasting*. Journal of Computational Physics, 227(7), 3572-3594.

4- Komen, G. J., Cavaleri, L., Donelan, M., Hasselmann, K., Hasselmann, S., & Janssen, P. A. E. M. (1996). *Dynamics and modelling of ocean waves*. Dynamics and Modelling of Ocean Waves, by GJ Komen and L. Cavaleri and M. Donelan and K. Hasselmann and S. Hasselmann and PAEM Janssen, pp. 554. ISBN 0521577810. Cambridge, UK: Cambridge University Press, August 1996, 554.

5-Tolman, H.L., 2014. W.I. development Group. *User manual and system documentation of WAVEWATCH III version 4.18 [No. 316]*. U. S. Department of Commerce National Oceanic and Atmospheric Administration National Weather Service National Centers for Environmental Prediction 5830 University Research Court College Park, MD 20740: Environmental Modeling Center Marine Modeling and Analysis Branch.

6- Delft, T. (2014). *SWAN User Manual Cycle III version 41.01*. Delft, Nederlands: Delft University of Technology Faculty of Civil Engineering and Geosciences Environmental Fluid Mechanics Section.

7-DHI. MIKE21. 2014. http://www.mikebydhi.com/products/mike-21.

8-Tomawac, 2014. *TOMAWAC wave model*, http://www.opentelemac.org/index. Php/modules-list/20-tomawac.

9- Rao, Y. H., Liang, S. X., & Yu, Y. X. (2012). *A method to determine the incident wave boundary conditions and its application*. China Ocean Engineering, 26(2), 205-216.

10- Moghaddam, E. I., Allahdadi, M. N., Hamedi, A., & Nasrollahi, A. (2018). *Wave-induced Currents in the Northern Gulf of Oman: A Numerical Study for Ramin Port along the Iranian Coast*. American Journal of Fluid Dynamics, 8(1), 30-39.

11- Ardani, S., & Soltanpour, M. (2015). *Modelling of sediment transport in Beris fishery port*. Civil Engineering Infrastructures Journal, 48(1), 69-82.

12- Pakhirehzan, M., Rahbani, M., & Malakooti, H. (2018). *Numerical Study of Winter Shamal Wind Forcing on the Surface Current and Wave Field in Bushehr's Offshore Using MIKE21*. IJCOE 2018, 2(2); p. 57-65.

13- Lavidas, G., & Venugopal, V. (2018). *Application of numerical wave models at European coastlines: A review*. Renewable and Sustainable Energy Reviews, 92, 489-500.

14- Becker, J. J., Sandwell, D. T., Smith, W. H. F., Braud, J., Binder, B., Depner, J. L., ... & Ladner, R. (2009). *Global bathymetry and elevation data at 30 arc seconds resolution: SRTM30_PLUS*. Marine Geodesy, 32(4), 355-371.

15- Badiei, P., & Siadat Mousavi, M. (2010). *The Third Generation Spectral Wave Model, WAVEWATACH-III, Enhanced for use in Nearshore Regions*. Civil Engineering Infrastructures Journal, 44(2), 289-302.

16- Jouon, A., Lefebvre, J. P., Douillet, P., Ouillon, S., & Schmied, L. (2009). *Wind wave measurements and modelling in a fetch-limited semi-enclosed lagoon*. Coastal engineering, 56(5-6), 599-608.

17- Smith, J. M., Hesser, T., Roland, A., & Bryant, M. (2018). *VALIDATION OF UNSTRUCTURED WAVEWATCH III FOR NEARSHORE WAVES.* Coastal Engineering Proceedings, 1(36), 55.

18-Sanil Kumar, V., & Muhammed Naseef, T. (2015). *Performance of ERA-Interim wave data in the nearshore waters around India*. Journal of Atmospheric and Oceanic Technology, 32(6), 1257-1269.

19-Mahjoobi, J., Etemad-Shahidi, A., & Kazeminezhad, M. H. (2008). *Hindcasting of wave parameters using different soft computing methods*. Applied Ocean Research, 30(1), 28-36.